Deficiency of gluconeogenic enzyme PCK1 promotes non-alcoholic steatohepatitis progression by activation of PI3K/AKT/PDGF axis

Qian Ye[1,#], Yi Liu[1,#], Guiji Zhang[1,#], Haijun Deng[1,#], Chang Chen[2], Xuanming Pan[1], Kang Wu[1], Jiangao Fan[3], Qin Pan[3], Kai Wang[1,*], Ailong Huang[1,*], Ni Tang[1,*]

[1]Key Laboratory of Molecular Biology for Infectious Diseases (Ministry of Education), Institute for Viral Hepatitis, Department of Infectious Diseases, The Second Affiliated Hospital, Chongqing Medical University, Chongqing, China

[2]Institute of Life Sciences, Chongqing Medical University, Chongqing, China

[3]Center for Fatty Liver, Department of Gastroenterology, Xin Hua Hospital Affiliated to Shanghai Jiao Tong University School of Medicine, Shanghai, China

[#]These authors contributed equally to this work.

***Corresponding author:**

Ni Tang, Ailong Huang, Kai Wang, Key Laboratory of Molecular Biology for Infectious Diseases (Ministry of Education), Institute for Viral Hepatitis, Department of Infectious Diseases, The Second Affiliated Hospital, Chongqing Medical University, Chongqing, China. Phone: 86-23-68486780, Fax: 86-23-68486780, E-mail: nitang@cqmu.edu.cn (N.T.), ahuang@cqmu.edu.cn (A.L.H.), wangkai@cqmu.edu.cn (K.W.)

Running title: PCK1 deficiency promotes NASH

Keywords:

phosphoenolpyruvate carboxykinase 1; gluconeogenesis; non-alcoholic steatohepatitis; PI3K/AKT pathway; platelet-derived growth factor AA

Abstract:

Background and Aims:

Nonalcoholic steatohepatitis (NASH) is a chronic liver disease characterized by hepatic lipid accumulation, inflammation, and progressive fibrosis. However, the pathomechanisms underlying NASH are incompletely explored. Phosphoenolpyruvate carboxykinase 1 (PCK1) catalyzes the first rate-limiting step of gluconeogenesis in the cytoplasm. This study was designed to determine the role of PCK1 in regulating NASH progression.

Methods:

Liver metabolism, hepatic steatosis, and fibrosis were evaluated at 24 weeks in liver-specific *Pck1*-knockout (L-KO) mice fed with NASH diet (high fat diet with *ad libitum* consumption of water containing glucose and fructose). AKT and RhoA inhibitors were evaluated for disease treatment in L-KO mice fed NASH diet.

Results:

PCK1 is downregulated in patients with NASH and mouse models of NASH.

L-KO mice displayed hepatic lipid disorder and liver injury fed with normal diet, while fibrosis and inflammation were aggravated when fed NASH diet. Mechanistically, transcriptome analysis revealed PCK1 deficiency upregulated genes involved in fatty acid transport and lipid droplet formation. Moreover, untargeted metabolomics analysis showed the accumulation of glycerol 3-phosphate, the substrate of triglyceride synthesis. Furthermore, the loss of PCK1 could activate the RhoA/PI3K/AKT pathway, which leads to increased secretion of PDGF-AA and promotes the activation of hepatic stellate cells. RhoA and AKT inhibitors alleviated NASH progression in L-KO mice fed NASH diet.

Conclusions:

PCK1 deficiency plays a key role in the development of hepatic steatosis and fibrosis by facilitating the RhoA/PI3K/AKT/PDGF-AA axis. These findings provide a novel insight into therapeutic approaches for the treatment of NASH.

Lay summary

Non-alcoholic steatohepatitis (NASH) is currently the most common chronic liver disease, which is correlated with progressing chronic disorder of lipid metabolism and a persistent inflammatory response. In the present study, decreased PCK1 is observed in patients with NASH and mouse NASH models, and its loss aggravates steatohepatitis in NASH mice fed high-fat, high-fructose diet by stimulating expression of lipogenic genes and lipid synthesis. Inhibitors of proteins involved in the underlying molecular process alleviated the liver disease, highlighting a new therapeutic strategy for NASH.

Graphical abstract

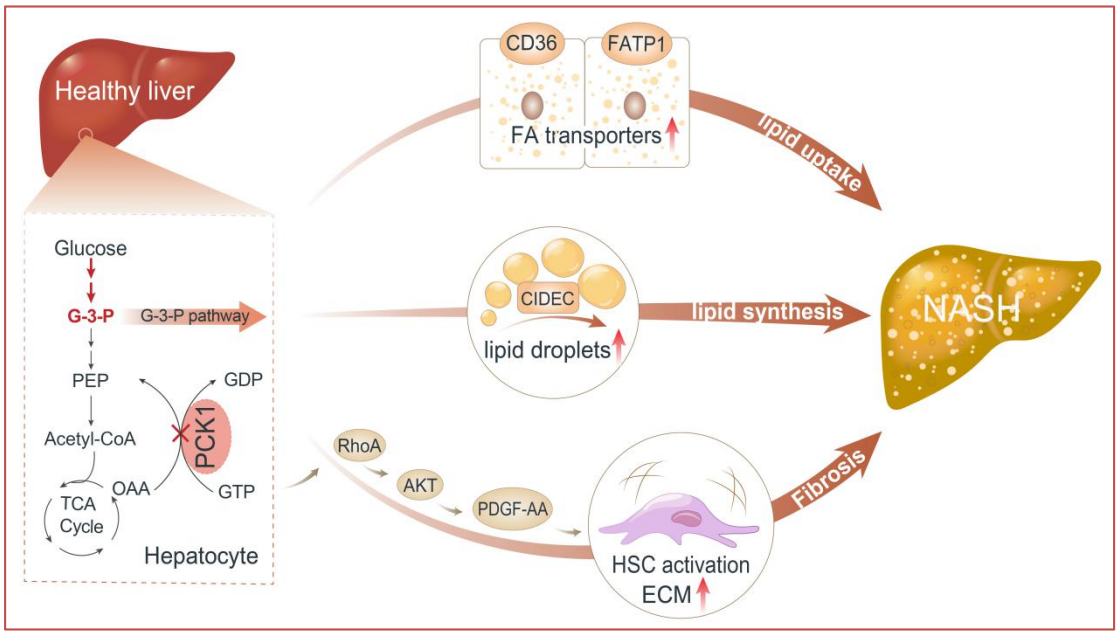

Highlights

• Gluconeogenic enzyme PCK1 is downregulated in both human patients and NASH mice.

• PCK1 depletion promotes hepatic steatosis by dysregulating lipid metabolism and synthesis.

• PCK1 loss promotes hepatic fibrosis by activating RhoA/PI3K/AKT/PDGF-AA axis.

• Targeting RhoA/AKT alleviates NASH progression in liver-specific *Pck1*-knockout mice.

Introduction

Non-alcoholic fatty liver disease (NAFLD) is the most common chronic liver disease worldwide affecting nearly 25% of U.S. and European adults.[1] NAFLD is characterized by aberrant lipid accumulation in hepatocytes in the absence of excessive alcohol consumption. NAFLD may progress to non-alcoholic steatohepatitis (NASH), a more serious form of liver damage hallmarked by irreversible pathological changes such as inflammation, varying degrees of fibrosis, and hepatocellular damage, which is more likely to develop into cirrhosis and hepatocellular carcinoma (HCC).[2] Although multiple parallel insults, including oxidative damage, endoplasmic reticulum stress, and hepatic stellate cell (HSC) activation have been proposed to explain the pathogenesis of NASH, the underlying mechanisms remain incompletely elucidated.[3]

Gluconeogenesis converts lipids and several other noncarbohydrate precursors into glucose, which occurs mainly in the liver to maintain glucose levels and energy homeostasis. Phosphoenolpyruvate carboxykinase 1 (PCK1) is the first rate-limiting enzyme in the gluconeogenesis pathway which converts oxaloacetate (OAA) to phosphoenolpyruvate (PEP) in the cytoplasm.[4] Our previous studies have shown that PCK1 deficiency promotes HCC progression by affecting glucose metabolism.[4] However, PCK1 has been found to regulate not only gluconeogenesis but also lipogenesis by activating sterol regulatory element binding proteins (SREBPs).[5] Patients lacking PCK1 function present

diffuse hepatic macrosteatosis concomitant with hypoglycemia and hyperlactacidemia.[6] Likewise, mice with reduced *Pck1* expression develop insulin resistance and exhibit hypoglycemia as well as hepatic steatosis, indicating an important role of PCK1 in regulating both glucose homeostasis and lipid metabolism.[7, 8] However, the exact role of PCK1 during NASH progression is incompletely understood.

The phosphoinositide 3-kinase/protein kinase B (PI3K/ATK) pathway plays a critical role in regulating cell growth and metabolism. This pathway can be activated in response to insulin, growth factors, energy, and cytokines, and in turn, regulates key metabolic processes, including glucose and lipid metabolism, as well as protein synthesis.[9] AKT promotes *de novo* lipogenesis (DNL) primarily through SREBP activation.[10] PI3K/AKT dysregulation leads to many pathological metabolic conditions, including obesity and type 2 diabetes.[11] NAFLD is characterized by disordered glucose and lipid metabolism in liver. However, although key to sensing metabolic stress, the exact role of the PI3K/AKT pathway in NAFLD/NASH progression is unclear.[12, 13]

In this study, we explored the role of Pck1 in a mouse NASH model. We unraveled the molecular mechanisms underlying disordered lipid metabolism, inflammation, and fibrosis induced by Pck1 depletion. We also delineated the functional importance of the PI3K/AKT pathway and its effectors in

steatohepatitis, providing a potential therapeutic strategy for treating NASH.

Material and Methods

Animal models

To generate liver-specific *Pck1*-knockout mice (L-KO), *Alb-Cre* mice were crossed with *Pck1*$^{loxP/loxP}$ mice. *Pck1*$^{loxP/loxP}$ mice from the same litter were used as controls (WT*).* Male WT and L-KO mice, 7–9-week-old, were fed NASH diet (Research Diets, D12492: 60% Kcal fat, with drinking water containing 23.1 g/L fructose and 18.9 g/L glucose) or a control chow diet (Research Diets, D12450J: 10% Kcal fat, with tap water) for 24 weeks. After male L-KO mice were fed with NASH diet for 16 weeks, they were divided into 3 groups and intraperitoneally injected with vehicle solution, MK2206 (AKT inhibitor) or Rhosin (RhoA inhibitor) for 8 weeks, respectively.

Details and other materials and methods are provided in the **Supplementary Materials**.

Results

PCK1 is downregulated in patients with NASH and mouse models of NASH

To determine whether PCK1 is involved in NAFLD, we first examined hepatic gene expression in a published transcriptome dataset (GEO: GSE126848) containing samples from 14 healthy, 12 obese, 15 NAFLD, and 16 NASH patients.[14] Bioinformatics analysis showed that 32 genes were significantly changed in obesity, NAFLD, and NASH; 12 genes were significantly downregulated and 20 genes were upregulated (Fig. S1A-C). Notably, *PCK1* was gradually reduced in obesity, NAFLD, and NASH patients (Fig. 1A). Downregulation of *PCK1* mRNA was also found in a similar dataset (GSE89632) (Fig. 1B). Next, we examined PCK1 expression in liver samples derived from NASH patients, NASH model mice, and *ob/ob* mice by q-PCR, immunoblotting, and immunohistochemistry. Both Pck1 mRNA and protein levels were significantly downregulated in the mice (Fig. 1C-G).

In addition, PCK1 mRNA and protein levels were downregulated in a dose-dependent manner during 24-hour palmitic acid (PA) stimulation (Fig. 1F and G), suggesting that transcription of PCK1 may be inhibited in response to lipid overload. We screened several known regulators of *PCK1* by q-PCR (Fig. S1D and E) and determined *AFT3*, a transcriptional repressor of *PCK1*[16], was upregulated upon PA stimulation (Fig. 1H). Similarly, ATF3 mRNA and protein levels were significantly upregulated in NASH and *ob/ob* mice (Fig. S1F and

G). Chromatin immunoprecipitation assays revealed that the binding of ATF3 to *PCK1* promoter was increased by PA administration (Fig. 1I). ATF3 knockdown restored the expression of PCK1 in human hepatocytes under PA treatment (Fig. 1J). Taken together, increased lipids caused upregulation of the repressor ATF3, impairing *PCK1* transcription in NASH patients and mouse models.

L-KO mice exhibit a distinct hepatic steatosis phenotype

To explore the functional role of *Pck1* in fatty liver disease, WT and L-KO mice were fed with chow diet for 24 weeks (Fig. 2A). From 16 weeks, L-KO mice showed increased body weight compared with WT mice (Fig. 2B), while there was no significant difference in the glucose tolerance test (GTT) and insulin tolerance test (ITT) (Fig. 2C and D). Moreover, significant hepatomegaly and increased liver weight were observed in L-KO mice (Fig. 2E). Alanine transaminase (ALT) and aspartate transaminase (AST) levels were higher in L-KO mice, indicating severe liver injury (Fig. 2F). In addition, total triglyceride (TG), total cholesterol (TC), and free fatty acids (FFAs) in liver tissues and serum were elevated in L-KO mice (Fig. 2G and H). Histochemistry and ELISA showed that L-KO mice exhibited prominent hepatic steatosis and higher levels of TNF-α (Fig. 2I and J). These data suggest that L-KO mice exhibited a distinct hepatic steatosis phenotype and liver injury even when fed normal chow.

Hepatic loss of *Pck1* promotes inflammation and fibrogenesis in NASH mice

To explore whether an unhealthy diet could exacerbate the pathologic changes in L-KO mice, WT and L-KO mice were fed with high fat diet with drinking water containing fructose and glucose (NASH diet) for 24 weeks (Fig. 3A). From 4 weeks, L-KO mice showed significant weight gain (Fig. 3B). GTT and ITT showed that L-KO mice developed a more severe form of glucose intolerance (Fig. 3C) and insulin resistance (Fig. 3D). L-KO mice had pale (Fig. 3E) and heavier livers (Fig. 3F), although there was no significant difference in liver weight ratio (Fig. S2A). Insulin, AST, ALT, TC, TG, and FFAs were increased in serum or liver homogenates of L-KO mice, suggesting more serious liver injury and lipid metabolism disorder (Fig. 3G, H; Fig. S2B and C). Analyses of L-KO liver sections revealed increased fat droplets, more severe fibrosis, and greater macrophage infiltration (Fig. 3I). Furthermore, L-KO mice had higher NAFLD activity score (NAS score) and higher TNF-α and IL-6 levels (Fig. 3J; Fig. S2G and H). q-PCR results showed that genes associated with lipid metabolism, fibrogenesis, and inflammatory infiltration were upregulated in L-KO mice (Fig. S2D-F). In summary, mice lacking hepatic *Pck1* showed substantial liver inflammation and fibrosis when fed NASH diet.

Transcriptomic and metabolomic analyses confirm loss of *Pck1* promotes lipid accumulation

To comprehensively investigate the role of *Pck1* in NASH, we performed RNA-seq analysis of liver samples from L-KO and WT mice fed normal chow or NASH diet for 24 weeks. Gene ontology analysis indicated that lipid metabolic processes were remarkably upregulated in L-KO mice fed with NASH diet (Fig. 4A). Volcano plot showed that genes involved in fatty acid transport, such as *Slc27a1* and *Cd36*, and lipid droplet synthesis, such as *Cidec* and *Cidea*, were upregulated in response to NASH diet (Fig. 4B). Gene Set Enrichment Analysis (GSEA) revealed that the PPAR signaling pathway was prominently upregulated in L-KO mice fed either diet (Fig. 4C; Fig. S3A and B). Several genes selected from the data set were independently validated by q-PCR and immunoblotting and found to be significantly overexpressed in L-KO mice (Fig. 4D and E). Furthermore, genes involved in the glycerol 3-phosphate (G3P) pathway were also overexpressed in L-KO mice (Fig 4F). Metabolomics analysis showed that compared with WT mice fed NASH diets, L-KO mice had significantly higher G3P and PA levels (Fig. 4G and H). Since G3P is a substrate for TG synthesis and PA is a key intermediate metabolite in DNL, these data suggested that *Pck1* ablation could promote the accumulation of lipid synthesis substrates.

To further examine the function of PCK1 on steatosis *in vitro*, we overexpressed (*PCK1*-OE) and knocked out PCK1 (*PCK1*-KO) in human

hepatocytes (Fig. S3C and D), and found that *PCK1*-OE attenuated the accumulation of lipid droplets, whereas *PCK1*-KO facilitated lipid accumulation (Fig. S3E and F). Collectively, these results suggested that hepatic *PCK1* deficiency leads to lipid accumulation by promoting the high expression of genes related to lipid metabolism and the accumulation of substrates related to lipid synthesis (Fig. S3G).

Hepatic *Pck1* deficiency leads to HSC activation via PI3K/AKT pathway

RNA-seq analysis indicated that the PI3K/AKT pathway was also specifically activated in L-KO mice fed NASH diet (Fig. 5A and B). Immunoblotting revealed p-AKT(S473) and p-AKT(T308), two activated forms of AKT, and downstream c-MYC were significantly upregulated in L-KO livers (Fig. 5C). q-PCR also confirmed the high expression of genes related to PI3K/AKT pathway in L-KO mice (Fig. S4A). Similarly, p-AKT(S473) and p-AKT(T308) significantly decreased in human *PCK1*-OE cells, but increased in *PCK1*-KO cells after 0.2 mM PA treatment (Fig. 5D and E).

To clarify the role of PI3K/AKT pathway activation, transcriptome data were further analyzed. Interestingly, *Col1a1*, *Col3a1,* and *Lama2*, which are primary components of the extracellular matrix (ECM), were upregulated as shown in the heat map of the PI3K/AKT pathway (Fig. S4B). Moreover, GSEA analysis revealed that ECM-receptor interaction was upregulated in L-KO mice (Fig. S4C). Since ECM deposition is usually considered the key event

underlying liver fibrosis, we suspected that activation of the PI3K/AKT pathway may promote fibrosis in L-KO mice. Considering HSCs are major ECM secretors, we performed human hepatocyte (MIHA) and HSC (LX-2) co-culture assays (Fig. 5F). Interestingly, q-PCR results showed that *ACTA2* (α-SMA, an HSC activation marker)*, COL1A1,* and *COL3A1* mRNA levels were increased in HSCs co-cultured with *PCK1*-KO cells, but were decreased in HSCs co-cultured with *PCK1*-OE cells (Fig. 5G and H). Likewise, COL1A1, COL3A1, and α-SMA expression was increased in liver tissues and primary HSCs of L-KO mice (Fig. 5I and J). This observation was confirmed by COL3A1 immunohistochemistry (Fig. 5K). However, these increases could be partially reversed by MK2206, an AKT inhibitor (Fig. 5L and M). Collectively, these data suggested that loss of PCK1 in hepatocytes induces HSCs activation and ECM formation via activating the PI3K/AKT pathway.

Paracrine PDGF-AA from hepatocytes promotes HSC activation

Hepatocytes elicit several fibrogenic actions in a paracrine fashion to promote the activation of HSCs,[17] and PCK1-mediated hepatic fibrosis may be involved in paracrine disorders. To test this hypothesis, several pro-fibrotic factors were screened, and *Pdgfa* was significantly elevated in liver tissues of L-KO mice (Fig. 6A). *Pdgfa* encodes a dimer disulfide-linked polypeptide (PDGF-AA), and the chronic elevation of PDGF-AA in mice liver induces fibrosis.[18] Immunoblotting and ELISA demonstrated increased PDGF-AA

expression in liver tissues and primary hepatocytes of L-KO mice (Fig. 6B-D). Moreover, PDGF-AA concentration was markedly increased in the culture medium of *PCK1*-KO cells (Fig. 6E), but decreased in that of *PCK1*-OE cells (Fig. 6F). Correspondingly, platelet-derived growth factor receptor alpha (*PDGFRα*), which encodes the PDGF-AA receptor, was increased in HSCs co-cultured with *PCK1*-KO cells, while decreased in HSCs co-cultured with *PCK1*-OE cells (Fig. 6G and H). To determine whether the pro-fibrogenic effect was mediated by PDGF-AA secretion, we used a neutralizing antibody against PDGF-AA. As expected, the increase of α-SMA, COL1A1, and COL3A1 in HSCs co-cultured with *PCK1*-KO cells can be reversed by anti-PDGF-AA (Fig. 6I).

Reviewing transcriptome data, we found that *Pdgfa* appeared in the heat map of the PI3K-AKT pathway (Fig. S4B). Immunohistochemistry demonstrated that p-AKT(S473) was positively correlated with PDGF-AA (Fig. 6J). The AKT inhibitor MK2206 significantly blocked the increase of PDGF-AA/PDGFA in the supernatants (Fig. 6K) and cells lysates (Fig. 6L) of *PCK1*-KO cells. Taken together, these data confirmed that PCK1 deficiency promoted the expression of PDGF-AA through the PI3K/AKT pathway, and activated HSCs through hepatocyte-HSC crosstalk.

PCK1 deficiency promotes the activation of the PI3K/AKT/PDGF-AA axis by activating RhoA signaling in hepatocytes

Rho GTPases, which cycle between active GTP-bound and inactive GDP-bound conformations, may activate the PI3K/AKT pathway.[19-21] Considering PCK1 catalyzes the conversion of OAA to PEP, consuming GTP to generate GDP (Fig 7A), we speculated that PCK1 deficiency may alter intracellular GTP homeostasis. To test this hypothesis, we examined several Rho GTPase protein levels in mice liver tissues and found that only inactivated RhoA (p-RhoA(S188)) was significantly reduced (Fig. 7B and C). Consistently, p-RhoA (S188) expression increased in *PCK1*-OE cells and decreased in *PCK1*-KO cells, and the effect was exacerbated by PA treatment (Fig. 7D). Rhosin was used to determine whether PI3K/AKT activation is dependent on RhoA. Immunoblotting, ELISA, and q-PCR showed that Rhosin blocked the increase of activated forms of AKT and PDGF-AA in *PCK1*-KO cell lysate and supernatant, as well as *ACTA2*, *COL1A1,* and *COL3A1* expression in HSCs co-cultured with *PCK1*-KO hepatocytes (Fig. 7E-G). Moreover, immunohistochemistry confirmed that PCK1 was positively correlated with p-AKT(S473) and PDGF-AA, and negatively related to p-RhoA(S188) in patient NASH samples (Fig. 7H). Taken together, these data indicate that PCK1 ablation stimulated the PI3K/AKT/PDGF-AA axis by activating RhoA GTPase.

Therapeutic treatment with RhoA and AKT inhibitors reduced progressive liver fibrosis *in vivo*

To explore whether blocking RhoA/PI3K/AKT could rescue the NASH phenotype in L-KO mice, Rhosin and MK2206 were used *in vivo* (Fig. 8A). Treatment of L-KO mice with Rhosin or MK2206 showed improved glucose intolerance (Fig. S5A) and insulin resistance (Fig. S5B). Furthermore, the increased liver weight was also prevented (Fig. 8B and C), whereas body weight was reduced only in the MK2206 treatment group (Fig. S5C). Additionally, Rhosin or MK2206 administration attenuated AST and ALT levels, as well as TG and FFA levels in serum and liver tissues (Fig. 8D; Fig. S5D and E). Similarly, histochemistry showed reduced liver steatosis, inflammation, and fibrosis in Rhosin or MK2206 treated mice (Fig. 8E), which was confirmed by measurement of liver TNF-α and IL-6 levels (Fig. 8F and G). Additionally, α-SMA, COL1A1, COL3A1, PDGF-AA, p-AKT(S473), and p-AKT(T308) expression were also decreased, while the expression of p-RhoA(S188) was increased (Fig. 8H). q-PCR results showed that the expression of genes related to inflammation and fibrosis were decreased after MK2206 or Rhosin treatment (Fig. 8I). These data suggested that the RhoA/PI3K/AKT axis plays a key role in NASH progression in L-KO mice.

Discussion

This study revealed that the hepatic gluconeogenic enzyme PCK1 plays an important role in the pathogenesis of NASH. The expression of PCK1 was diminished in livers from patients or mice with NASH. Moreover, deletion of PCK1 significantly exacerbated hepatic steatosis, fibrosis, and inflammation in mouse models fed NASH diet. Mechanistically, loss of PCK1 not only promotes steatosis by enhancing lipid deposition, but also induces fibrosis by HSC activation via the PI3K/AKT/PDGF-AA axis, thus promoting the progression of NASH.

Abnormal lipid metabolism is a characteristic of NAFLD and NASH. Previous studies assumed that disturbance of lipid metabolism was usually caused by abnormal expression of genes related to lipid metabolism.[22] However, recent studies have demonstrated that disruption of glucose metabolism also leads to abnormal lipid metabolism. Deficiency of fructose-1,6-bisphosphatase 1 (FBP1) and glucose-6-phosphatase catalytic subunit (G6PC), key enzymes of the gluconeogenic pathway, results in severe hepatic steatosis and hypoglycemia, indicating that abnormal glucose metabolism could also disrupt lipid homeostasis.[23, 24] As the first rate-limiting enzyme in gluconeogenesis pathway, it is currently not clear whether PCK1 plays a critical role in NAFLD/NASH development. In this study, we identified a robust decrease in PCK1 expression in the livers of obese mice and NAFLD/NASH patients, causing

severe hepatic steatosis and confirming that disordered glucose metabolism can affect lipid metabolism.

PCK1 was reported to be regulated transcriptionally, as well as post-translationally, such as by acetylation, phosphorylation, and ubiquitination.[25, 26] Our study showed *PCK1* mRNA levels were reduced. We identified *ATF3*, a member of the bZIP family of transcription factors, transcriptionally repressed *PCK1* upon PA overload. ATF3 has been shown to function as a transcriptional repressor in stress and nutrient-deprived responses and was upregulated in NAFLD patients and mouse model.[15, 27, 28] Ethanol was found to inhibit the transcription of *PCK1* by stimulating the expression of ATF3.[29] Our findings identified a direct link between transcriptional factor ATF3 and downregulated *PCK1* expression in a NASH model.

Previous studies using PCK1 agonists or whole-body *Pck1* knockdown mice have verified that PCK1 may affect lipid metabolism.[30, 31] In the present study, we found that liver-specific *Pck1* knockout induced significant hepatic steatosis even under normal feeding conditions. This is a very important phenomenon, since it is uncommon for a single gene ablation to cause spontaneous steatosis unless a high fat diet is used. Moreover, we observed that *Pck1* L-KO accompanied by a high-fat high-fructose diet promotes not only steatosis, but

also inflammation and fibrosis by upregulating proinflammatory molecules such as TNF-α and IL-6. However, a previous study found that whole-body *Pck1* knockdown alleviates hepatic inflammation in NAFLD mouse model.[32] We speculate that this discrepancy is possibly due to differences between diet plan and animal models.

Lipid accumulation is the essence of steatosis. Emerging evidence has indicated that increased fatty acid uptake is associated with lipid accumulation.[33, 34] In this study, genes involved in fatty acid uptake such as *Cd36* and *Slc27a1* were highly expressed in L-KO mice. In addition, *Cidec,* a lipid droplet-associated protein that promotes their formation, was increased by both chow and NASH diets, and recently it was claimed to upregulated in NALFD patients and mice, suggesting that PCK1 ablation also promotes lipid droplet formation.[35, 36] Abnormal levels of metabolites also contribute to TG accumulation in liver. The G3P pathway contributes to over 90% of TG synthesis.[37] Since our metabolomics data showed that G3P and PA were significantly upregulated in L-KO mice, we propose that PCK1 deficiency promotes hepatic lipid accumulation by enhancing the expression of *Cd36*, *Slc27a1,* and *Cidec* and the levels of metabolic substrates such as G3P and PA. However, the exact mechanism by which PCK1 regulates G3P pathway and the expression levels of *Cd36*, *Slc27a1* remains to be further explored.

Fibrosis is another characteristic of NASH and drives the transition from simple steatosis to NASH. Activation of HSCs through the secretion of profibrotic cytokines, such as TGF-β and PDGF, is a key event in liver fibrosis.[2] A recent study identified high mobility group protein B1 (HMGB1), secreted by FBP1-deficient hepatocytes, as the main mediator to activate HSCs, showing the important crosstalk between hepatocytes and HSCs via paracrine signaling.[24] Herein, we found that PDGF-AA was secreted by PCK1-deficient hepatocytes and acted in a paracrine manner to activate HSCs. Increased deposition of extracellular matrix and activation of HSCs were shown in PDGFA-transgenic mice, however, the underlying mechanism mediating PDGF-AA upregulation in fibrosis remains unclear.[18] Here, we demonstrated that PCK1 deficiency promoted PDGF-AA secretion via activation of the RhoA/PI3K/AKT pathway. Mechanistically, we hypothesize that PCK1 deletion increases intracellular GTP levels, thus promoting RhoA function and further activating the PI3K/AKT pathway. Based on our *in vitro* findings, we used pharmacological AKT and RhoA inhibitors, MK2206 and Rhosin respectively, in L-KO NASH mice. Hepatic steatosis, fibrosis, and inflammation were significantly attenuated in treated mice. Although RhoA and AKT inhibitors are currently only in phase 3 trials or preclinical studies for the treatment of liver fibrosis or clinical tumors, these compounds may also have a promising therapeutic potential for NASH.[38-40]

In conclusion, this study demonstrated that hepatic PCK1 deficiency could promote lipid deposition and fibrosis in murine NASH. Moreover, hepatic PCK1 loss activates the RhoA/PI3K/AKT pathway, which increases secretion of PDGF-AA and promotes HSC activation. RhoA inhibitors MK2206 and Rhosin could reduce progressive liver fibrosis, providing a therapeutic window for NASH treatment.

Abbreviations:

AKT, protein kinase B; ALT, Alanine transaminase; AST, aspartate transaminase; α-SMA, alpha-smooth muscle actin (ACTA2); ATF3, Activating Transcription Factor 3; bZIP, Basic Leucine Zipper Domain; ChIP, chromatin immunoprecipitation; CIDEC and CIDEA, cell death inducing DFFA like effector C and A; COL1A1, COL1A3, recombinant collagen type I alpha 1 and alpha 3; CD36, fatty acid translocase; DNL, *de novo* lipogenesis; FFA, free fatty acid; G3P, glycerol 3-phosphate; GTT, glucose tolerance test; GSEA, Gene Set Enrichment Analysis; HE, hematoxylin and eosin; ITT, insulin tolerance test; Lama2, laminin subunit alpha 2; L-KO, liver-specific *Pck1*-knockout mice; NASH, non-alcoholic steatohepatitis; NAFLD, non-alcoholic fatty liver disease; NAS, NAFLD activity score; PCK1, Phosphoenolpyruvate carboxykinase 1; PCK1, Phosphoenolpyruvate carboxykinase 1; PDGF-AA, platelet-derived growth factor AA; PI3K,

phosphatidylinositol 3-kinase; PPAR, Peroxisome Proliferator-Activated Receptor; RhoA, Ras homolog family member A; SLC27A1, solute carrier family 27 member 1; TC, total cholesterol; TG, Triglyceride

Acknowledgements

We would like to thank Dr. T.-C He (University of Chicago, USA) and Prof. Ding Xue (Tsinghua University, China) for providing the pAdEasy system and CRISPR/Cas9 system, respectively. We thank Prof. Youde Cao and Yalan Wang (Chongqing Medical University, China) for providing samples and pathological analysis support. We are grateful to Prof. Xi Li (Chongqing Medical University, China) for providing us liver tissue samples of *ob/ob* mice. This work was supported by the China National Natural Science Foundation (grant no. U20A20392, 82073251, 82072286, 81872270), the 111 Project (No. D20028), the Natural Science Foundation Project of Chongqing (cstc2018jcyjAX0254, cstc2019jscx-dxwtBX0019, cstc2019jcyj-msxmX0587), the Major National S&T program (2017ZX10202203-004), the Leading Talent Program of CQ CSTC (CSTCCXLJRC201719), the Science and Technology Research Program of Chongqing Municipal Education Commission (KJZD-M202000401, KJQN201900429, CY200406), the Kuanren talents program of the second affiliated hospital of Chongqing Medical University, and the Scientific Research Innovation Project for Postgraduate in Chongqing (grant nosCYB19168, CYS19193).

Conflict of interest:

The authors declare no competing interests.

Author contributions:

NT, AH, and KW conceived and designed the study. QY, YL and GZ performed most experiments and analyzed the data. HD and KW conducted bioinformatics analysis. XP assisted with mice experiments. CC performed metabolic detection. JF and QP provided NAFLD/NASH human samples. QY, KW, and NT wrote the manuscript with all authors providing feedback.

Reference

[1] Younossi Z, Anstee QM, Marietti M, Hardy T, Henry L, Eslam M, et al. Global burden of NAFLD and NASH: trends, predictions, risk factors and prevention. Nature reviews Gastroenterology & hepatology 2018;15:11-20.

[2] Schuster S, Cabrera D, Arrese M, Feldstein AE. Triggering and resolution of inflammation in NASH. Nature reviews Gastroenterology & hepatology 2018;15:349-364.

[3] Arab JP, Arrese M, Trauner M. Recent Insights into the Pathogenesis of Nonalcoholic Fatty Liver Disease. Annual review of pathology 2018;13:321-350.

[4] Tuo L, Xiang J, Pan X, Hu J, Tang H, Liang L, et al. PCK1 negatively regulates cell cycle progression and hepatoma cell proliferation via the AMPK/p27(Kip1) axis. Journal of experimental & clinical cancer research : CR 2019;38:50.

[5] Xu D, Wang Z, Xia Y, Shao F, Xia W, Wei Y, et al. The gluconeogenic enzyme PCK1 phosphorylates INSIG1/2 for lipogenesis. Nature 2020;580:530-535.

[6] Santra S, Cameron JM, Shyr C, Zhang L, Drögemöller B, Ross CJ, et al. Cytosolic phosphoenolpyruvate carboxykinase deficiency presenting with acute liver failure following gastroenteritis. Molecular genetics and metabolism 2016;118:21-27.

[7] She P, Shiota M, Shelton KD, Chalkley R, Postic C, Magnuson MA.

Phosphoenolpyruvate carboxykinase is necessary for the integration of hepatic energy metabolism. Mol Cell Biol 2000;20:6508-6517.

[8] Millward CA, Desantis D, Hsieh CW, Heaney JD, Pisano S, Olswang Y, et al. Phosphoenolpyruvate carboxykinase (Pck1) helps regulate the triglyceride/fatty acid cycle and development of insulin resistance in mice. Journal of lipid research 2010;51:1452-1463.

[9] Hoxhaj G, Manning BD. The PI3K-AKT network at the interface of oncogenic signalling and cancer metabolism. Nat Rev Cancer 2020;20:74-88.

[10]Porstmann T, Griffiths B, Chung YL, Delpuech O, Griffiths JR, Downward J, et al. PKB/Akt induces transcription of enzymes involved in cholesterol and fatty acid biosynthesis via activation of SREBP. Oncogene 2005;24:6465-6481.

[11] Huang X, Liu G, Guo J, Su Z. The PI3K/AKT pathway in obesity and type 2 diabetes. International journal of biological sciences 2018;14:1483-1496.

[12] Chen J, Chen J, Huang J, Li Z, Gong Y, Zou B, et al. HIF-2α upregulation mediated by hypoxia promotes NAFLD-HCC progression by activating lipid synthesis via the PI3K-AKT-mTOR pathway. Aging 2019;11:10839-10860.

[13] Chi Y, Gong Z, Xin H, Wang Z, Liu Z. Long noncoding RNA lncARSR promotes nonalcoholic fatty liver disease and hepatocellular carcinoma by promoting YAP1 and activating the IRS2/AKT pathway. Journal of translational medicine 2020;18:126.

[14] Suppli MP, Rigbolt KTG, Veidal SS, Heebøll S, Eriksen PL. Hepatic

transcriptome signatures in patients with varying degrees of nonalcoholic fatty liver disease compared with healthy normal-weight individuals. Am J Physiol Gastrointest Liver Physiol 2019;316:G462-g472.

[15] Fang J, Ji YX, Zhang P, Cheng L, Chen Y, Chen J, et al. Hepatic IRF2BP2 Mitigates Nonalcoholic Fatty Liver Disease by Directly Repressing the Transcription of ATF3. Hepatology 2020;71:1592-1608.

[16] Allen-Jennings AE, Hartman MG, Kociba GJ, Hai T. The roles of ATF3 in liver dysfunction and the regulation of phosphoenolpyruvate carboxykinase gene expression. The Journal of biological chemistry 2002;277:20020-20025.

[17] Kucukoglu O, Sowa JP, Mazzolini GD, Syn WK, Canbay A. Hepatokines and adipokines in NASH-related hepatocellular carcinoma. Journal of hepatology 2020;5:S0168-8278(20)33746-6.

[18] Thieringer F, Maass T, Czochra P, Klopcic B, Conrad I, Friebe D, et al. Spontaneous hepatic fibrosis in transgenic mice overexpressing PDGF-A. Gene 2008;423:23-28.

[19] Higuchi M, Masuyama N, Fukui Y, Suzuki A, Gotoh Y. Akt mediates Rac/Cdc42-regulated cell motility in growth factor-stimulated cells and in invasive PTEN knockout cells. Current biology : CB 2001;11:1958-1962.

[20] Dou C, Liu Z, Tu K, Zhang H, Chen C, Yaqoob U, et al. P300 Acetyltransferase Mediates Stiffness-Induced Activation of Hepatic Stellate Cells Into Tumor-Promoting Myofibroblasts. Gastroenterology 2018;154:2209-2221.e2214.

[21] Calvayrac O, Mazières J. The RAS-related GTPase RHOB confers resistance to EGFR-tyrosine kinase inhibitors in non-small-cell lung cancer via an AKT-dependent mechanism. EMBO Mol Med 2017;9:238-250.

[22] Snaebjornsson MT, Janaki-Raman S, Schulze A. Greasing the Wheels of the Cancer Machine: The Role of Lipid Metabolism in Cancer. Cell metabolism 2020;31:62-76.

[23] Sanders FW, Griffin JL. De novo lipogenesis in the liver in health and disease: more than just a shunting yard for glucose. Biological reviews of the Cambridge Philosophical Society 2016;91:452-468.

[24] Li F, Huangyang P, Burrows M, Guo K, Riscal R. FBP1 loss disrupts liver metabolism and promotes tumorigenesis through a hepatic stellate cell senescence secretome. Nat Cell Biol 2020;22:728-739.

[25] Chakravarty K, Cassuto H, Reshef L, Hanson RW. Factors that control the tissue-specific transcription of the gene for phosphoenolpyruvate carboxykinase-C. Critical reviews in biochemistry and molecular biology 2005;40:129-154.

[26] Wang Z, Dong C. Gluconeogenesis in Cancer: Function and Regulation of PEPCK, FBPase, and G6Pase. Trends in cancer 2019;5:30-45.

[27] Hai T, Wolfgang CD, Marsee DK, Allen AE, Sivaprasad U. ATF3 and stress responses. Gene expression 1999;7:321-335.

[28] Tu C, Xiong H, Hu Y, Wang W, Mei G, Wang H, et al. Cardiolipin Synthase 1 Ameliorates NASH Through Activating Transcription Factor 3 Transcriptional

Inactivation. Hepatology 2020.

[29] Tsai WW, Matsumura S, Liu W, Phillips NG, Sonntag T, Hao E, et al. ATF3 mediates inhibitory effects of ethanol on hepatic gluconeogenesis. Proceedings of the National Academy of Sciences of the United States of America 2015;112:2699-2704.

[30] Gut P, Baeza-Raja B, Andersson O, Hasenkamp L, Hsiao J, Hesselson D, et al. Whole-organism screening for gluconeogenesis identifies activators of fasting metabolism. Nature chemical biology 2013;9:97-104.

[31] Hakimi P, Johnson MT, Yang J, Lepage DF, Conlon RA, Kalhan SC, et al. Phosphoenolpyruvate carboxykinase and the critical role of cataplerosis in the control of hepatic metabolism. Nutrition & metabolism 2005;2:33.

[32] Satapati S, Kucejova B, Duarte JA, Fletcher JA, Reynolds L, Sunny NE, et al. Mitochondrial metabolism mediates oxidative stress and inflammation in fatty liver. The Journal of clinical investigation 2015;125:4447-4462.

[33] Miquilena-Colina ME, Lima-Cabello E, Sánchez-Campos S, García-Mediavilla MV, Fernández-Bermejo M, Lozano-Rodríguez T, et al. Hepatic fatty acid translocase CD36 upregulation is associated with insulin resistance, hyperinsulinaemia and increased steatosis in non-alcoholic steatohepatitis and chronic hepatitis C. Gut 2011;60:1394-1402.

[34] Doege H, Grimm D, Falcon A, Tsang B, Storm TA, Xu H, et al. Silencing of hepatic fatty acid transporter protein 5 in vivo reverses diet-induced non-alcoholic fatty liver disease and improves hyperglycemia. J Biol Chem

2008;283:22186-22192.

[35] Langhi C, Baldán Á. CIDEC/FSP27 is regulated by peroxisome proliferator-activated receptor alpha and plays a critical role in fasting- and diet-induced hepatosteatosis. Hepatology 2015;61:1227-1238.

[36] Xu MJ, Cai Y, Wang H, Altamirano J, Chang B, Bertola A, et al. Fat-Specific Protein 27/CIDEC Promotes Development of Alcoholic Steatohepatitis in Mice and Humans. Gastroenterology 2015;149:1030-1041.e1036.

[37] Alves-Bezerra M, Cohen DE. Triglyceride Metabolism in the Liver. Comprehensive Physiology 2017;8:1-8.

[38] Chien AJ, Tripathy D, Albain KS, Symmans WF, Rugo HS, Melisko ME, et al. MK-2206 and Standard Neoadjuvant Chemotherapy Improves Response in Patients With Human Epidermal Growth Factor Receptor 2-Positive and/or Hormone Receptor-Negative Breast Cancers in the I-SPY 2 Trial. Journal of clinical oncology : official journal of the American Society of Clinical Oncology 2020;38:1059-1069.

[39] Schmid P, Abraham J, Chan S, Wheatley D, Brunt AM, Nemsadze G, et al. Capivasertib Plus Paclitaxel Versus Placebo Plus Paclitaxel As First-Line Therapy for Metastatic Triple-Negative Breast Cancer: The PAKT Trial. Journal of clinical oncology : official journal of the American Society of Clinical Oncology 2020;38:423-433.

[40] Yoon C, Cho SJ, Aksoy BA, Park DJ, Schultz N, Ryeom SW, et al.

Chemotherapy Resistance in Diffuse-Type Gastric Adenocarcinoma Is Mediated by RhoA Activation in Cancer Stem-Like Cells. Clinical cancer research : an official journal of the American Association for Cancer Research 2016;22:971-983.

Figures and figure legends

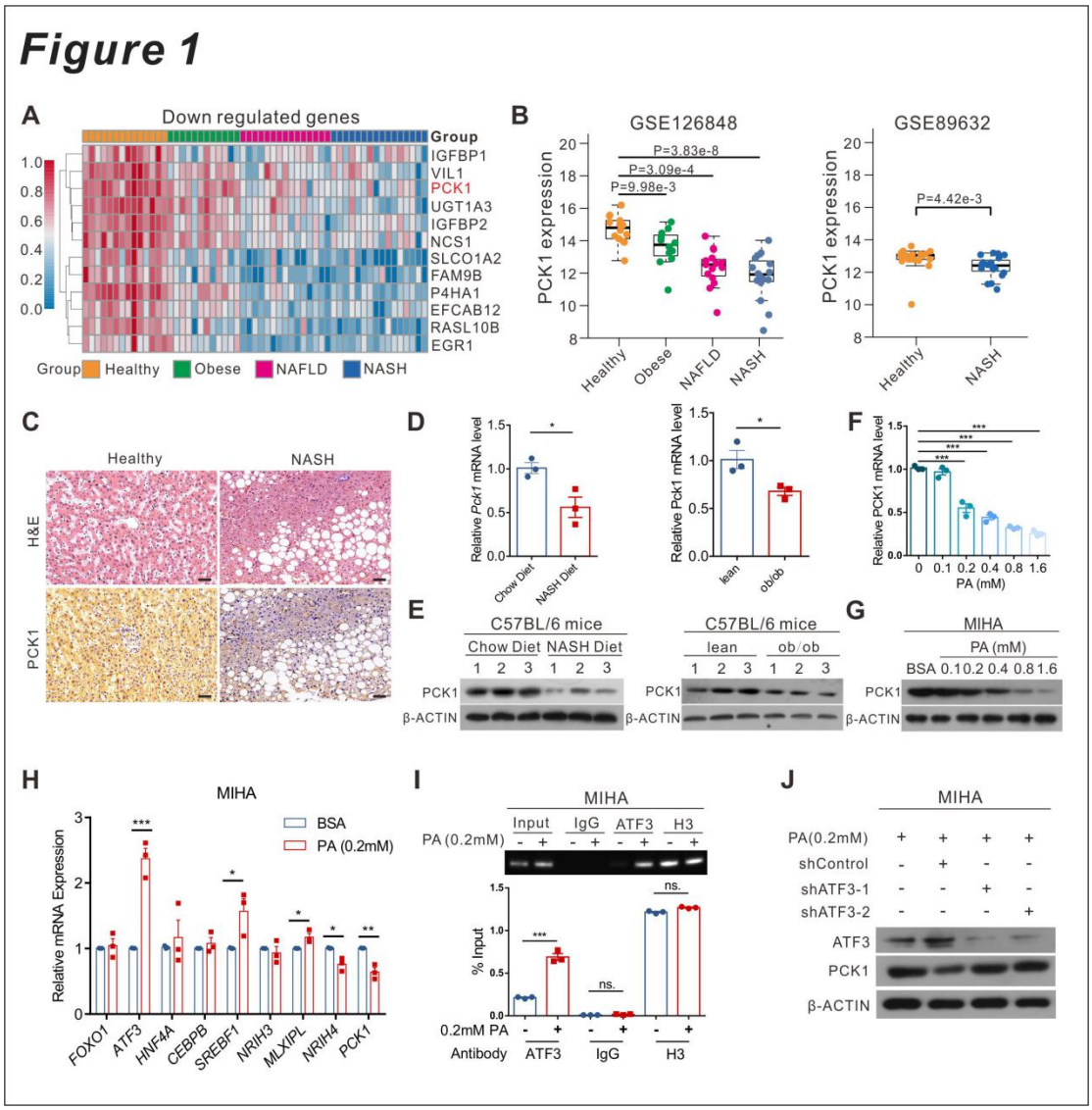

Fig. 1. PCK1 is downregulated in patients with NASH and mouse models of NASH. (A) Genes downregulated in patients with obesity (n=12), NAFLD (n=15), and NASH (n=16) from GSE126848 dataset. (B) Relative *PCK1* mRNA levels in GSE126848 and GSE89632 datasets. (C) PCK1 expression in normal individuals and patients with NASH. Scale bars: 50 μm. (D-E) mRNA and protein levels of PCK1 in the livers of WT mice fed with NASH diet and *ob/ob* mice (n=3 per group). (F-G) PCK1 mRNA and protein levels in MIHA cells with

palmitic acid (PA) or BSA. (H) Relative levels of indicated genes in MIHA cells treated with 0.2 mM PA. (I) ChIP assays were performed in MIHA cells with or without PA treatment using an antibody against ATF3, IgG or H3. (J) Protein levels of PCK1 in MIHA cells infected with either shControl or shATF3 treated with 0.2 mM PA. Data expressed as mean ± SEM. *P < 0.05, ** P < 0.01, ***P < 0.001.

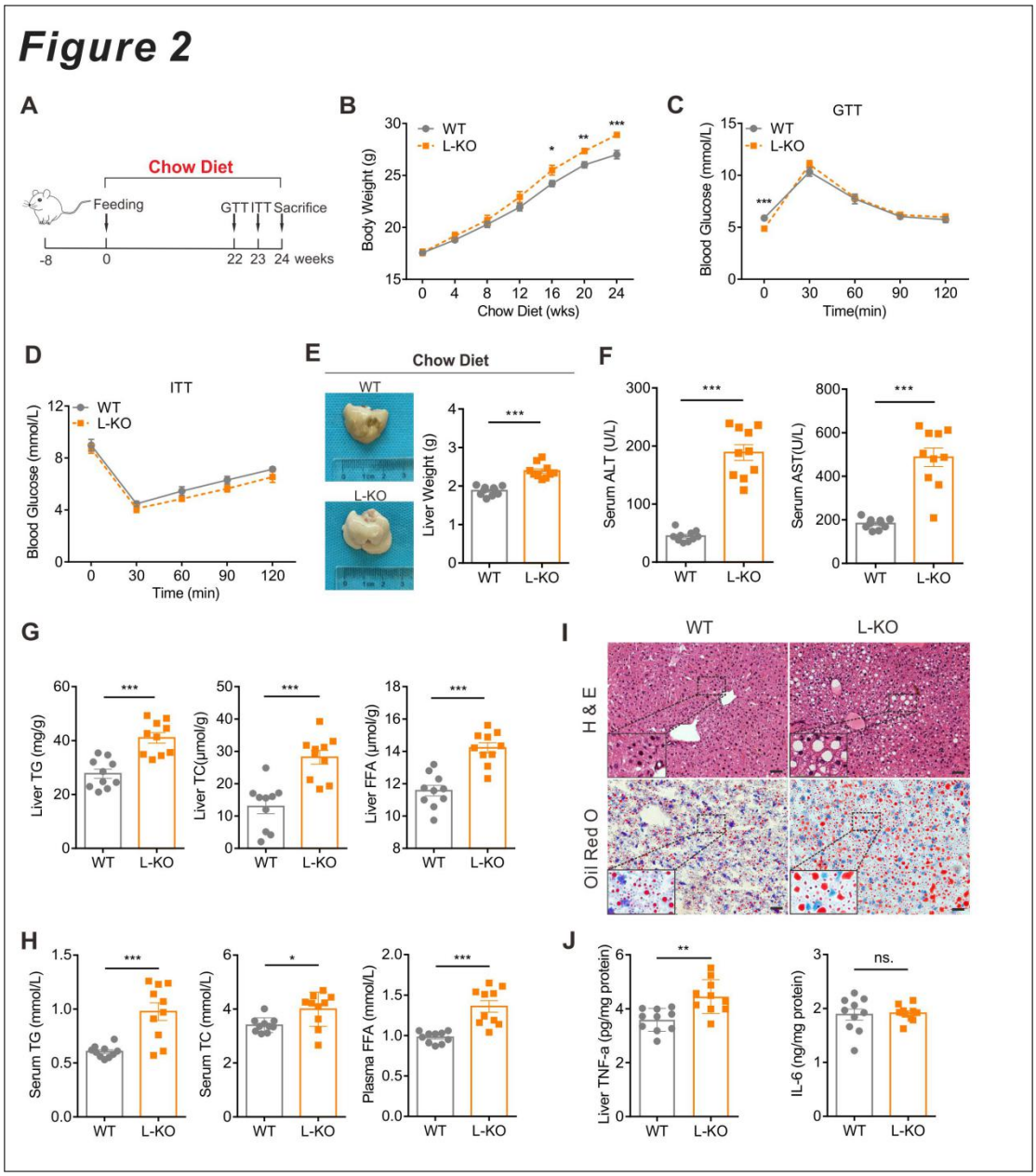

Fig. 2. L-KO mice fed chow diet exhibit a distinct hepatic steatosis phenotype. (A) Schematic diagram of mouse model fed with chow diet. Body weight (B), GTT (C), and ITT (D) were measured in WT and L-KO mice. (E) Representative liver image and liver weight of WT and L-KO mice. (F-H) Determination of ALT, AST, TG, TC and FFA levels in serum or liver tissues. (I) Paraffin-embedded liver sections were stained with HE, and frozen sections were stained with Oil Red O. Scale bars: 50 μm. (J) Levels of TNF-α, lL-6 in liver tissues. Data expressed as mean ± SEM.; *P < 0 .05, ** P < 0.01, ***P < 0.001.

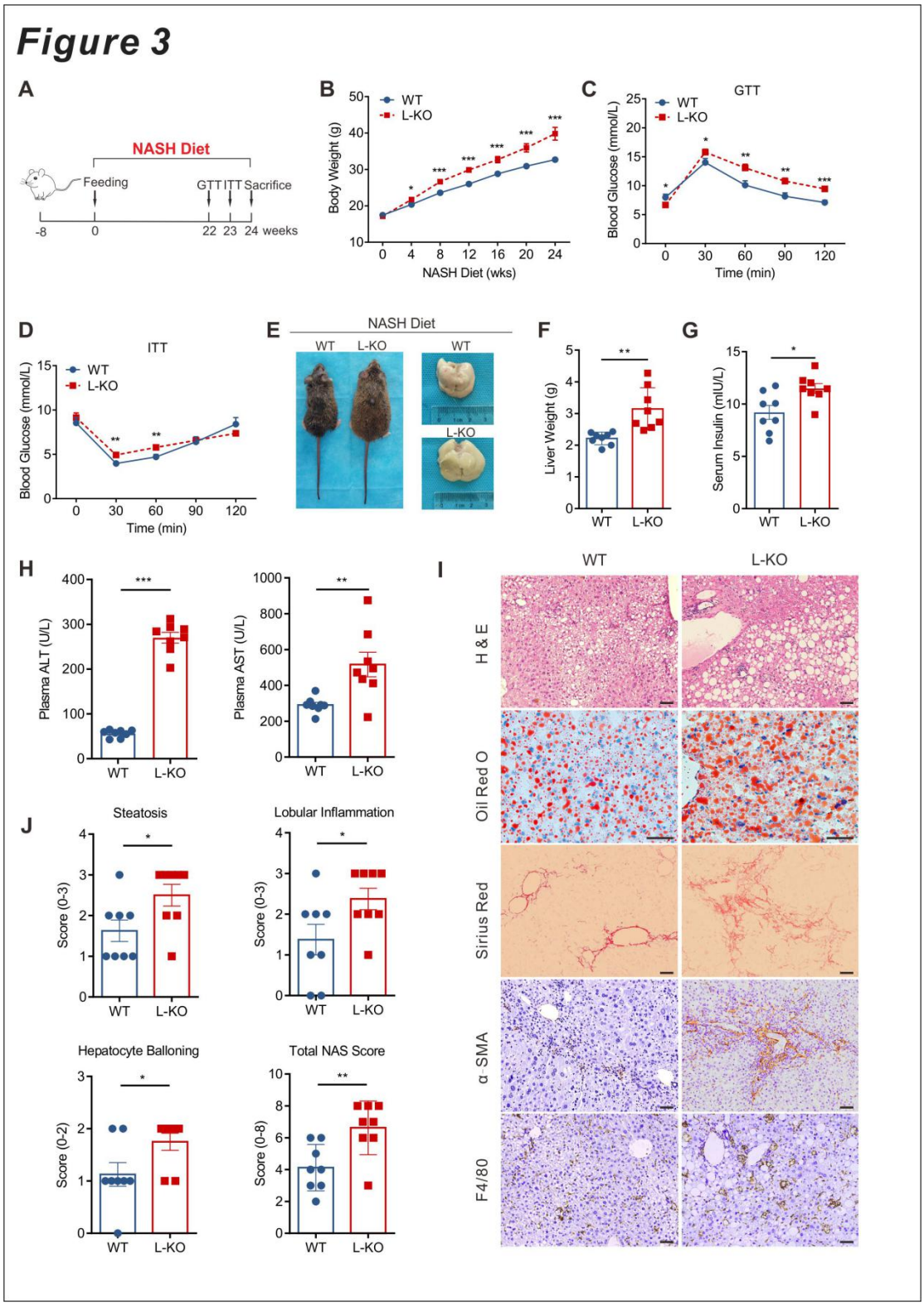

Fig. 3. PCK1 ablation accelerates inflammation and fibrogenesis in NASH model. (A) Schematic diagram of mouse model fed with NASH diet. Body weight (B), GTT (C), and ITT (D) were measured in WT and L-KO mice. (E)

Representative gross liver morphology and whole body photo. (F) Liver weight, serum levels of (G) insulin, (H) ALT and AST were measured. (I) Paraffin-embedded liver sections were stained with HE, Sirius Red, α-SMA and F4/80. Frozen sections stained with Oil Red O. Scale bars: 50 μm. (J) NAS scores of each group. Data expressed as mean ± SEM; *P < 0.05, ** P < 0.01, ***P < 0.001.

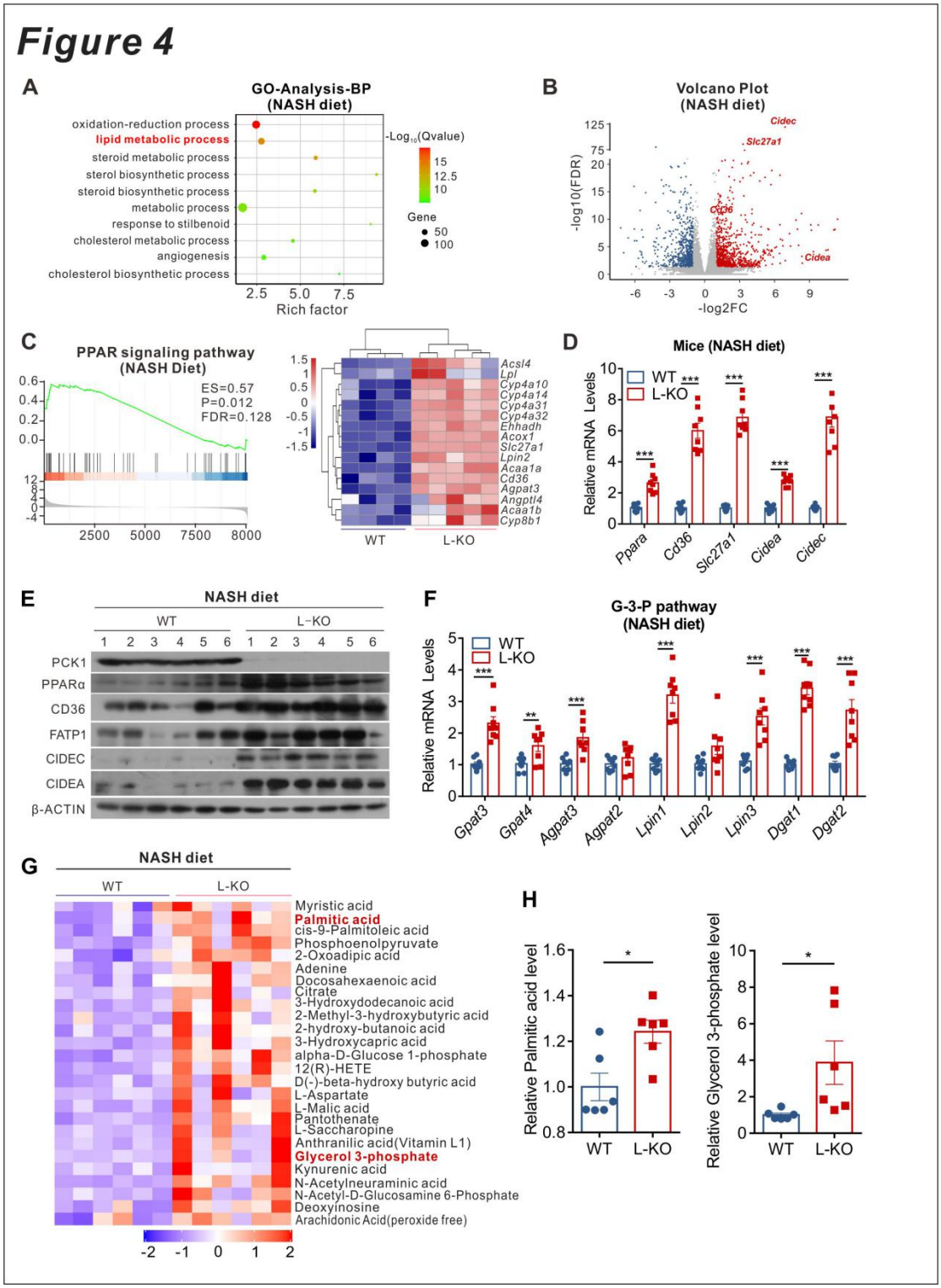

Fig. 4. Loss of PCK1 promotes lipid accumulation confirmed by transcriptome and metabolome. RNA sequencing was performed on livers of WT and L-KO mice fed NASH diet. (A) Gene ontology analysis of all significantly changed genes in top 10 biological processes. (B) Volcano plot

representation of significantly up- and downregulated genes. (C) GSEA plot (left) of enrichment in “PPAR signaling pathway” signature; Heatmap (right) presentation of significantly upregulated PPAR target genes. (D-E) q-PCR and immunoblot analysis of indicated genes or protein expression in mice liver tissues. (F) Relative mRNA expression of key genes in G3P pathway. (G) Upregulated metabolites detected by untargeted metabolomics (n=6). (H) The relative level of G3P and PA in mice liver tissues. Data expressed as mean ± SEM.; *P < 0.05, **P < 0.01, ***P < 0.001.

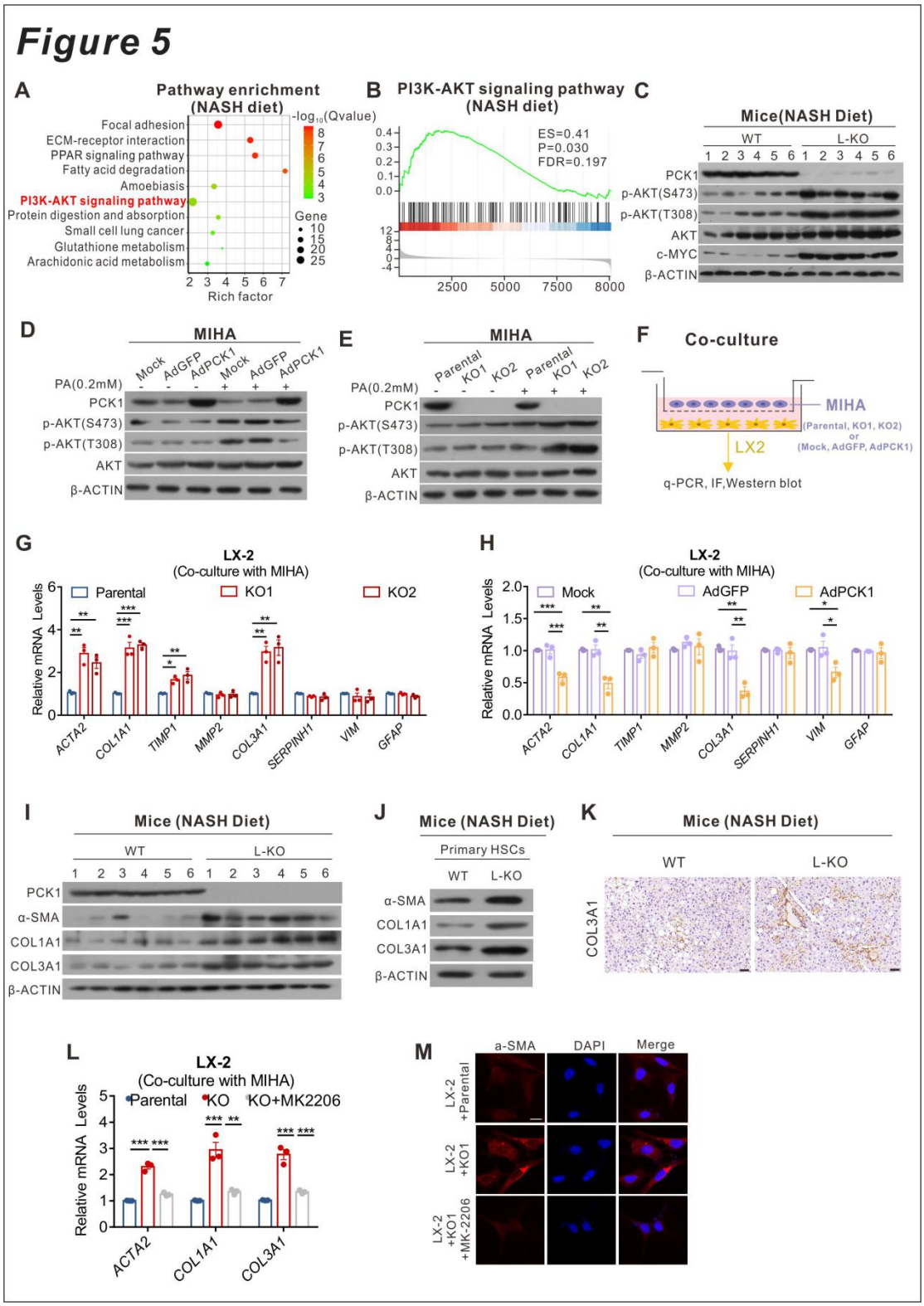

Fig. 5. Hepatic PCK1 deficiency leads to HSC activation via PI3K/AKT pathway. (A) Pathway enrichment analysis of significantly upregulated genes in L-KO mice. (B) GSEA plot of enrichment in PI3K/AKT pathway. (C-E)

Immunoblot analysis of AKT, p-AKT(S473), p-AKT(T308) in mice liver tissues or *PCK1*-OE and *PCK1*-KO MIHA cells with or without 0.2 mM PA treatment. (F) Schematic flow chart of co-culture models. (G-H) q-PCR analysis of fibrosis related gene in HSC LX-2 cells co-cultured with *PCK1*-KO or *PCK1*-OE MIHA cells. (I and J) Western blot of fibrosis related gene/protein in liver tissues or primary HSCs. (K) COL3A1 immunostaining in mice liver sections. Scale bars: 50 μm. (L-M) Immunofluorescence images and relative mRNA expression of *ACTA2*/α-SMA, *COL1A1* and *COL3A1* in LX-2 cells co-cultured with *PCK1*-KO MIHA cells treated with AKT inhibitor MK2206 (10 μM). Data expressed as mean ± SEM.; *P < 0.05, **P < 0.01, ***P < 0.001.

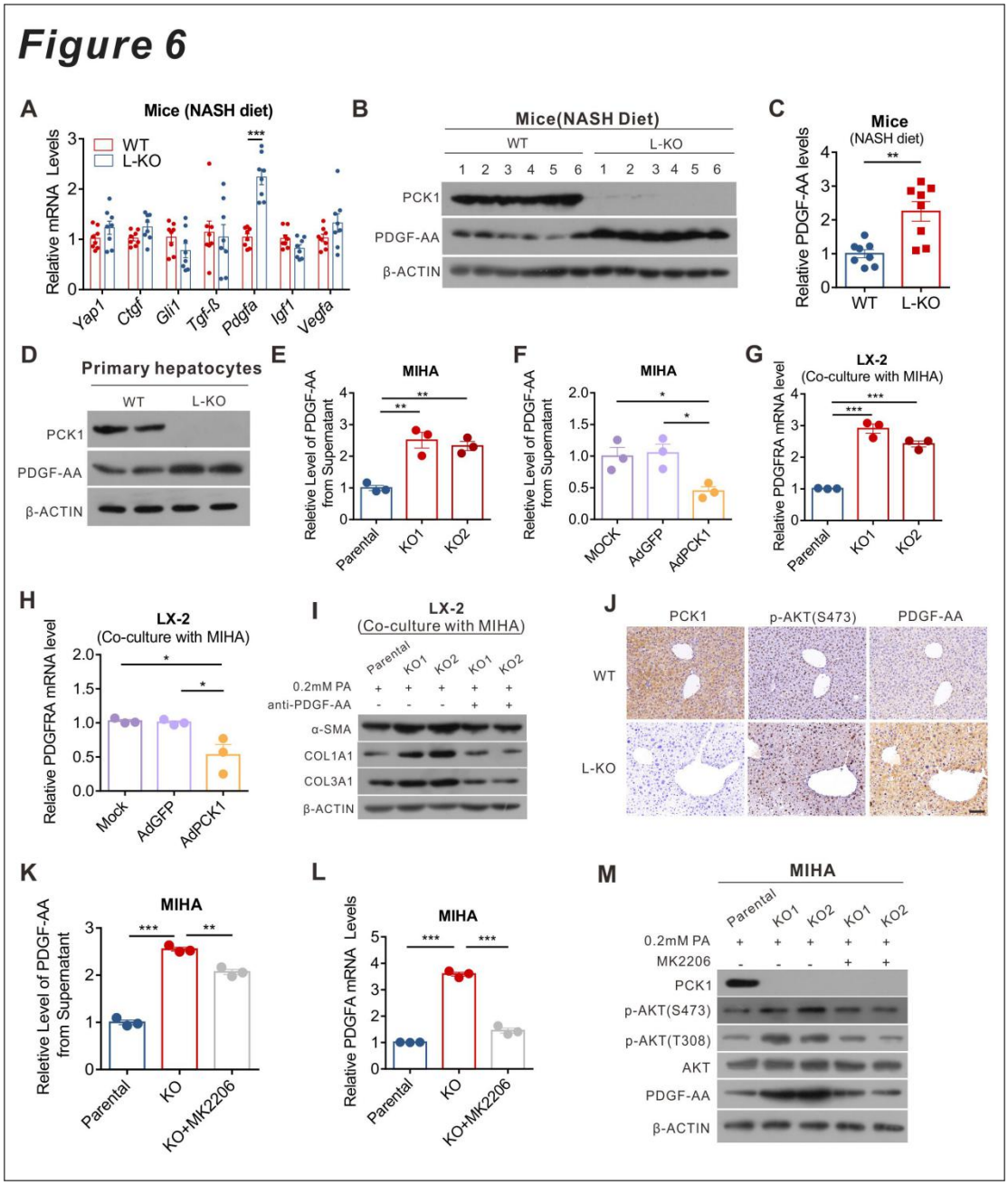

Fig. 6. Paracrine PDGF-AA from hepatocytes promotes HSC activation.

(A) Expression levels of genes related to fibrogenesis. PDGF-AA protein levels in liver tissue detected by Western blot (B) and ELISA (C). (D) PDGF-AA protein levels in primary hepatocytes. (E-F) Secreted PDGF-AA levels in the conditional medium of *PCK1*-KO or *PCK1*-OE MIHA cells. (G-H) mRNA levels of *PDGFRA* in cell lysate of LX-2 co-cultured with *PCK1*-KO or *PCK1*-OE

MIHA cells. (I) Indicated protein level in LX-2 cells co-cultured with *PCK1*-KO MIHA cells containing nonspecific rabbit IgG or a PDGF-AA blocking antibody. (J) Immunohistochemistry for PCK1, p-AKT(S473) and PDGF-AA in mice liver sections. Scale bars: 50 μm. (K-L) Levels of PDGF-AA or *PDGFA* in the conditional medium or cell lysate of *PCK1*-KO MIHA cells treated with AKT inhibitor MK2206 (10 μM). (G) Indicated protein levels in *PCK1*-KO MIHA cells treated with AKT inhibitor MK2206 (10 μM). Data expressed as mean ± SEM.; *P < 0.05, **P < 0.01, ***P < 0.001.

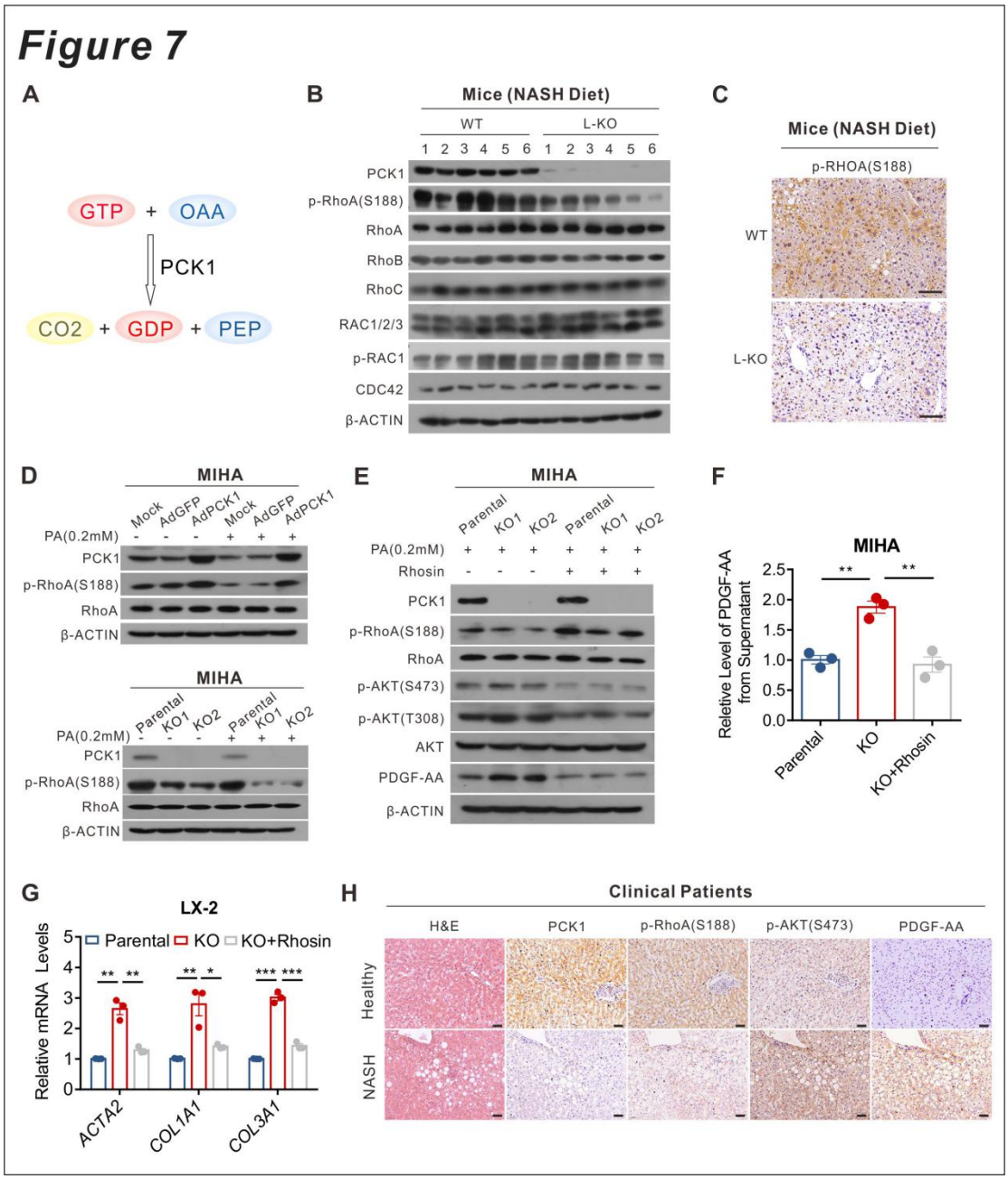

Fig. 7. PCK1 deficiency promotes the activation of PI3K/AKT/PDGF-AA axis by activating RhoA in hepatocytes. (A) Schematic representation of catalytic function of PCK1. (B) Immunoblotting analysis of indicated protein in mice liver tissues. (C) p-RhoA immunohistochemistry of mice liver tissues. Scale bars: 50 μm. (D) Immunoblots of p-RhoA(S188) and RhoA in *PCK1*-OE and *PCK1*-KO MIHA cells with or without 0.2 mM PA treatment. (E) Expression

of indicated proteins in *PCK1*-KO MIHA cells after addition of Rhosin (30 μM). (F) Levels of PDGF-AA in the supernatant of *PCK1*-KO MIHA cells treated with Rhosin (30 μM). (G) Relative mRNA expression of *ACTA2*, *COL1A1*, and *COL3A1* in LX-2 cells co-cultured with *PCK1*-KO MIHA cells treated with Rhosin (30 μM). (H) Immunohistochemistry for PCK1, p-RhoA(S188), p-AKT(S473), and PDGF-AA in normal individuals and patients with NASH. Scale bars: 50 μm. Data expressed as mean ± SEM.; *P < 0.05, **P < 0.01, ***P < 0.001.

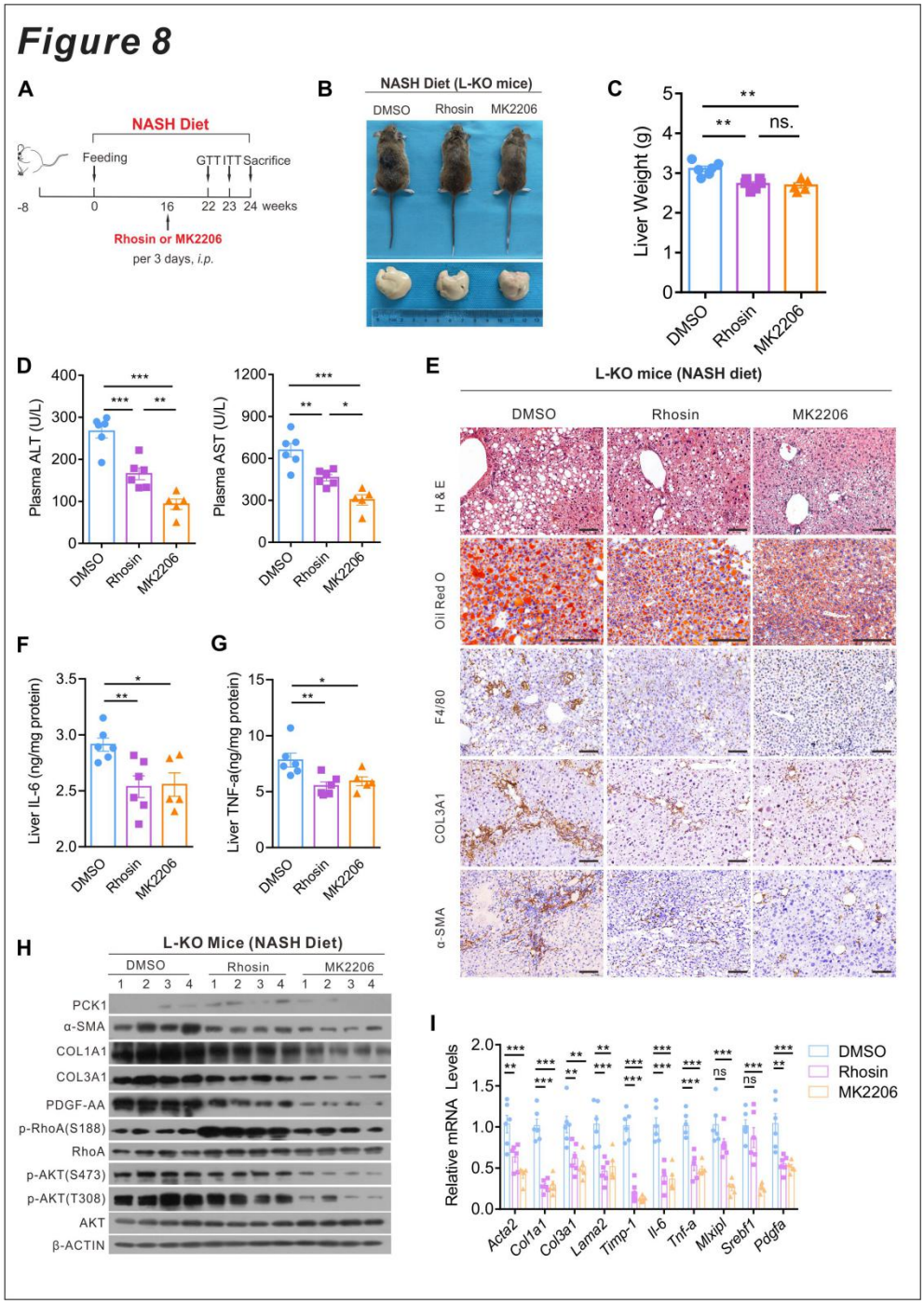

Fig. 8. AKT and RhoA inhibitors prevent the development of NASH *in vivo.* L-KO mice were fed NASH diet for 24 weeks, and therapeutic treatment with AKT or RhoA inhibitor was initiated at 16 weeks. (A) Schematic diagram of L-KO mice treated with Rhosin or MK2206. (B) Representative whole body and gross liver morphology. (C) Liver weight (right), and (D) serum ALT and AST. (E)

Paraffin-embedded liver sections were stained with HE and F4/80 or immunostained for COL3A1 and α-SMA. Frozen sections stained with Oil Red O. Scale bars: 50 μm. (F-G) Levels of TNF-α, lL-6 in liver tissues. (H) Expression of indicated protein in mice liver tissues. (I) mRNA levels of genes associated with lipid metabolism, fibrogenesis, and inflammatory infiltration. Data expressed as mean ± SEM; *P < 0.05, ** P < 0.01, ***P < 0.001.